NACA

RESEARCH MEMORANDUM

FLIGHT INVESTIGATION OF LOADS ON A BUBBLE-TYPE CANOPY

By

Cloyce E. Matheny and Wilber B. Huston

Langley Aeronautical Laboratory
Langley Field, Va.

NATIONAL ADVISORY COMMITTEE
FOR AERONAUTICS

WASHINGTON

October 29, 1948

NACA RM No. L8C30

NATIONAL ADVISORY COMMITTEE FOR AERONAUTICS

RESEARCH MEMORANDUM

FLIGHT INVESTIGATION OF LOADS ON A BUBBLE-TYPE CANOPY

By Cloyce E. Matheny and Wilber B. Huston

SUMMARY

The results of pressure-distribution measurements obtained in flight over the free-blown canopy of a fighter-type airplane are presented. The measurements were obtained on the same canopy previously tested in the Langley full-scale tunnel in order to determine the degree of correlation between flight and wind-tunnel results and the effects of Mach number and distortion on the pressure distribution. The measurements show that for comparable conditions there is good agreement between flight and wind-tunnel results for both the internal and external pressure coefficients. It is shown that Mach number has a greater effect upon vertical load coefficient than on either the fore and aft or side load coefficients. Within the limit of the tests, the effect of Mach number is independent of lift coefficient. The over-all effect of opening the canopy is to reduce the external negative pressure coefficients and, in general, to reduce the external loads. For the canopy tested, the effects of distortion appear to be small.

INTRODUCTION

As a result of several failures of canopies during flight, the Bureau of Aeronautics, Department of the Navy, requested the Langley Laboratory of the National Advisory Committee for Aeronautics to conduct a general investigation to determine the critical loading conditions for representative canopy types. The first part of this investigation was to include the measurement of the pressure distribution for three representative canopy types in the Langley full-scale tunnel over a wide range of operating conditions of power, yaw, lift coefficient, and canopy position. The canopy types investigated are the single sliding, front and rear sliding, and bubble types, and the results are reported in references 1, 2, and 3, respectively.

A second part of the investigation was to consist of flight measurements over one or two of the canopies tested to determine the degree of correlation between full-scale-tunnel results and those from flight and to determine the severity of the effects of Mach number and distortion. The present paper gives flight results of the pressure measurements over

the bubble-type canopy. A brief indication is given of how the results may be extended beyond the scope of the flight tests to calculate loads on the canopy.

SYMBOLS

q	dynamic pressure, pounds per square foot
C_L	airplane lift coefficient
p_i	internal static pressure in cockpit, pounds per square foot
p	external pressure over canopy, pounds per square foot
p_o	free-stream static pressure, pounds per square foot
P	external pressure coefficient $\left(\frac{p - p_o}{q}\right)$
P_i	internal pressure coefficient $\left(\frac{p_i - p_o}{q}\right)$
C_x, C_y, C_z	drag, side, and vertical external load coefficients, respectively $\left(\text{for example, } C_x = \frac{L_{x_e}}{qA}\right)$
C_{z_L}	vertical load coefficient due to attitude
$\Delta C_{z_{T_c}}$	increment in vertical load coefficient due to thrust coefficient
ΔC_{z_M}	increment in vertical load coefficient due to Mach number
C_{m_z}	vertical external moment coefficient about leading edge of canopy
g	acceleration due to gravity, feet per second per second
ρ	mass density of air, slugs per cubic foot
V	true airspeed, feet per second
V_e	equivalent airspeed, miles per hour $\left(V\sigma^{1/2}\right)$

M	Mach number
D	diameter of propeller, feet
T	thrust, pounds
T_c	thrust coefficient $\left(\frac{T}{\rho V^2 D^2}\right)$
L_x, L_y, L_z	drag, side, and vertical net load, respectively, pounds
Q	torque, pound-feet
Q_c	torque coefficient $\left(\frac{Q}{\rho V^2 D^3}\right)$
h	pressure altitude, feet
A	maximum cross-sectional area of canopy transverse to longitudinal axis, 2.66 square feet
C_p	center of pressure of canopy $\left(\frac{-C_{m_z}}{C_z}\right)$

Subscripts:

e	external
i	internal
l	left
r	right

APPARATUS

Airplane and engine.- The airplane used in these tests (fig. 1) was a single-seated Navy fighter. With the exception of an airspeed boom which was mounted on the right wing, there were no external modifications to the airplane.

The airplane was powered by a Pratt & Whitney R-2800-34W engine having a normal rated power of 2100 brake horsepower at sea level for 2800 rpm driving a four-blade Aeroproducts propeller. The propeller-engine gear ratio was 0.45 to 1. The propeller was 12 feet 7 inches in diameter having blades number H20C-162-11M5 with an activity factor of 106.2.

Canopy.- The canopy was a free-blown production model (fig. 2) and was the same one used in the full-scale-tunnel tests with the exception that the size of orifices and tubing installed for test purposes were made larger to minimize lag effects. The plexiglass part of the canopy was made from a sheet 1/4 inch thick.

Instrumentation.- Standard NACA instrumentation was used to measure airspeed, altitude, acceleration, time, and static pressure at various locations on the airplane. The external static pressures on the canopy were measured by means of 52 flush-type orifices arranged in six rows transverse to the longitudinal axis and six additional orifices for spot checks along the line of symmetry. (See fig. 3.) Pressure tubes of $\frac{1}{8}$-inch inside diameter connected each orifice with the recording manometer. The pressure lines were from 8 to 12 feet in length. Two additional cells were used, one to record reference pressure in rear part of the fuselage with respect to the pressure at the static holes of the pitot-static tube and the other to record pressure in the cockpit with respect to the pressure in the rear part of the fuselage. The static-pressure orifice in the cockpit was located slightly less than shoulder height and to the left of the pilot's seat.

TESTS

Insofar as possible the tests were arranged to obtain pressure distribution data that would (1) be comparable to full-scale-tunnel results, (2) indicate Mach number effects, and (3) indicate distortion effects.

The majority of the flight tests consisted of pull-ups at various speeds at an altitude of about 10,000 feet. For speeds below 190 miles per hour, the tests were made with the canopy closed, 3 inches open, half open, and full open (18 in.). With the canopy in the closed position the tests were continued to a maximum Mach number of 0.717. The sideslip angle was not measured because in reference 3 it will be noted that with small angles of sideslip the effect on the distribution is small.

A group of tests were also made in level flight at two widely separated altitudes in order to give a wide range of thrust-coefficient value.

In order to determine the effects of distortion of the canopy on the pressure distribution, a series of tests were made at the same Mach number and attitude but at widely separated altitudes.

The flight tests were made with the ventilators open and the propeller operating at the conditions of thrust and torque shown in figure 4 calculated for normal rated power for the powered flights and with the throttle fully closed for the power-off tests.

At the higher Mach numbers the tests could not be carried to so high values of lift coefficient as were obtained in the tunnel because of the operating limitations of the airplane. In some instances, therefore, comparisons could not be made at exactly the same lift coefficients.

METHODS AND RESULTS

The individual point pressures acting on the canopy surface were first reduced to pressure coefficient form and plotted in the plane of the six transverse sections shown in figure 3. In each case the pressure coefficients P and P_i were referenced to true free-stream static pressure. (See symbols for definition.) The results are shown in figures 5 to 8. Figure 5(a) shows the power-off distributions for four canopy positions at a lift coefficient of 1.18. Figure 6(a) shows the power-on distributions for four canopy positions at a lift coefficient of 0.50. Figures 5(b) and 6(b) are comparable distributions obtained from full-scale-tunnel measurements. Similar symbols and line segments have been used for various canopy positions for clarity in the comparisons. Figure 7 presents distributions obtained with the canopy closed for four Mach numbers ranging from 0.30 to 0.71 with power on and a lift coefficient of about 0.2. Figure 8 presents pressure distributions obtained at a Mach number of 0.67 and a lift coefficient of about 0.2 at about 10,000 and 28,000 feet pressure altitude. This figure is included to show the effects of distortion for the canopy in the closed position.

The pressure measured within the canopy during the various tests was reduced to an internal pressure coefficient P_i. The results are shown in figure 9.

From plots of the type shown in figures 5 to 8 the point pressures were summed to obtain the load coefficient acting vertically C_z, the fore and aft load coefficient C_x, the load coefficient on each half of the canopy C_{y_l}, C_{y_r}, and the side load coefficient C_y. The process for reducing the data used was mainly one of numerical integration in which the summation of the products of the local pressure coefficient and its effective projected area was taken. Stray points could not be readily detected with the numerical method; therefore, a running plot of point pressure coefficient against airplane lift coefficient was made for each orifice. Since the curves obtained were straight lines below the critical Mach number, errors could be immediately detected. Even with these auxiliary plots it was found that the method was considerably shorter in this case than mechanical integration.

The values of the external load coefficients determined in this manner are given in figures 10 and 11. Figure 10 shows the external load coefficient as a function of the airplane lift coefficient for both

power off and power on and for four canopy positions and a Mach number of about 0.30. A similar plot for Mach numbers ranging from 0.50 to 0.71 is presented in figure 11 for the canopy in the closed position and for power on.

The associated internal load coefficients are presented in figures 12 and 13. These coefficients were determined by methods similar to those for determining the external load coefficient. Figure 12 gives values of the internal load coefficient at a Mach number of about 0.3 as a function of airplane lift coefficient for all canopy positions and both power off and power on. The load coefficients associated with the higher Mach numbers are presented in figure 13 with power on and canopy closed.

DISCUSSION

Comparison with Wind-Tunnel Tests

The pressure distributions measured in flight at low speeds confirm the principal features noted in the full-scale-tunnel tests. Partly opening the canopy reduced the magnitude of the external negative pressure coefficients and increased the internal negative pressure coefficients, increasing the lift coefficient caused a small increase in the magnitude of the external pressure coefficients, and the high axial velocities and rotation of the slipstream at high thrust conditions increased the magnitude of the pressure coefficients and produced asymmetry in the distribution of pressure.

This confirmation of the wind-tunnel results and the degree of correlation between flight and full-scale-tunnel measurements is illustrated by the pressure distributions shown in figures 5 and 6. Power-off results at $C_L = 1.18$ are shown in figures 5(a) and 5(b). Quantitative agreement exists at all four canopy positions shown, even though the wind-tunnel tests were made with the propeller removed at a Mach number less than 0.1 and the flight tests were made with the propeller windmilling at $M = 0.3$. Slipstream effects are illustrated in figure 6 at $C_L = 0.50$. The asymmetrical change in the magnitude of the pressure coefficients is more marked in figure 6(b) than in figure 6(a) since the value of T_c in the wind-tunnel tests is larger than that in the flight tests. This difference in the value of T_c accounts for the fact that the peak negative pressure coefficients obtained in the full-scale-tunnel tests are higher than those obtained in flight for the first three stations. Stations downwind from the maximum radius are less affected by the thrust differences.

A comparison of the internal pressure coefficients obtained in flight, power off, with the results obtained in the full-scale tunnel is given in figure 14. Although the same canopy was used in both cases the wind-tunnel

tests were made on a different airplane. Internal canopy pressure is a function not only of the pressure distribution over the airplane but also of the area and location of the various leaks between the interior and exterior. With the canopy closed the values of pressure coefficient agree within ±0.05, even though two different airplanes were used and the cockpit ventilator was open in the flight tests but closed in the wind-tunnel tests. As shown in reference 4, closing the ventilator will reduce the cockpit pressure by $0.07q_c$ with the canopy closed. With the canopy open the differences between test conditions would be expected to be of less influence, which as shown in figure 14 is the case for the two intermediate positions. For the fully opened position, the difference between flight and wind-tunnel tests is chiefly the result of the different locations used for the static-pressure orifice. In the flight tests the orifice was fixed at the pilot's shoulder, whereas in the tunnel the orifice was fixed with respect to the canopy. The values obtained from the full-scale tunnel are believed more representative than the flight values.

Mach Number and Distortion

In order to give a quantitative measure of the effects of Mach number and distortion and to establish a basis for calculating canopy loads, it is convenient first to examine the load coefficients (especially C_z) as influenced by canopy position, lift coefficient, and power.

Effect of canopy position.- It may be seen from figures 9 and 12 that as the canopy is opened 3 inches the pressure in the cockpit rapidly drops as indicated by the change in load coefficient C_{z_i} from a value of 0.15 to a value of 1.53. The pressure continues to drop as the canopy is opened further until a value of 1.65 is reached with the canopy about half open. With further opening of the canopy the pressure rises until $C_{z_i} = 1.3$ at the full-open position. The particular variation measured may be associated with the fact that for small canopy openings the interior is subjected to the low-pressure field at the opening with the configuration remaining essentially the same. At the larger openings, however, the configuration is changed and other factors such as protruding edges and slight angles of yaw may affect the result.

The effect of canopy movement on the external pressures for both flight and full-scale-tunnel measurements illustrated in figures 5 and 6 is to reduce the negative pressure over all but the last two stations. At these stations no definite trend may be seen. The change in the magnitude of the external pressure coefficients is in the direction to reduce the pressure differential between the inner and outer surfaces of the canopy. The external load coefficients (see fig. 10) show, as would be expected, the over-all reduction in the magnitude of the pressure coefficient associated with opening the canopy.

Effect of lift coefficient.- The results shown in figures 10 and 11 for the external load coefficients and in figures 12 and 13 for the internal load coefficients indicate a linear increase with airplane lift coefficient. This variation is in line with the indications obtained from the auxiliary plots which showed point pressures to vary linearly with airplane lift coefficient.

Effect of power.- From the pressure distributions it was observed that power has an influence on the general level of the pressures measured. For sections ahead of the maximum radius the negative pressures are increased while behind this station the effect is to reduce the negative pressures. The over-all increase may be noted in figure 10 where it is shown that the values for powered flight are above those for the power-off conditions. The dissymmetry introduced by power is most easily seen from examination of figures 10 and 14. In figure 10 it may be noted that the values of C_Y for the power-on condition, regardless of side, are larger numerically than those for no power although the resultant is quite small and varies linearly with thrust coefficient as may be noted from figure 14.

From figure 12 it appears that the internal load coefficients did not vary with power condition within the limits of the experimental error.

Effect of Mach number and distortion.- The pressure distributions given in figure 7 for the canopy-closed position indicate that as the Mach number is changed from 0.30 to 0.71 at constant lift coefficient the point pressures over the forward two stations are increased, whereas for the pressures over the after sections no consistent variation may be noted. As shown in figure 11, the vertical load coefficient C_z and to a lesser extent the coefficients C_{y_l} and C_{y_r} which are obtained from the consideration of the pressure coefficients on each half of the canopy show a variation with Mach number. In figures 7 and 11 Mach number effects are linked with variations in the value of T_c; therefore, the results of figure 10 have been used to correct the load coefficient C_z to the condition for $T_c = 0$ for several lift coefficients. The corrected variation is given in figure 15 where it may be seen that the change in load coefficient C_z with M is independent of the lift coefficient for the range given. It may be noted that had it been possible to give the distributions of figure 7 on the basis of equal or zero T_c the difference would have been larger than that shown.

The flight results obtained with this canopy agree qualitatively as regards Mach number effects with those reported in reference 5 for canopy X-1 which is similar to the one tested.

From figure 8 it is seen that in spite of a large variation in dynamic pressure (208 to 466 lb/sq ft) any distortion causes changes which appear to be within the experimental error of the data.

Extension of Results Beyond Scope of Tests

Although the tests carried out in connection with the program on the flight test airplane did not cover the full range of the design V–n diagram, the data obtained enable some extension beyond the range tested so that some discussion of the critical loads may be made. In this connection the results for the vertical load coefficient C_z given in figures 10, 12, 15, and 16 together with the following equation defining the vertical load

$$L_z = qA \left[\left(C_{z_L} + \Delta C_{z_{T_c}} + \Delta C_{z_M}\right) - C_{z_i}\right]$$

have been found to be useful. The value of C_{z_L} is available from figure 10 for the appropriate canopy position for zero power. The increment in coefficient due to thrust coefficient is available from figure 16 for the various canopy positions. The increment in load coefficient due to Mach number can be obtained from figure 15. Corrections for Mach number are only available above $M = 0.3$ for the canopy-closed condition since operation with canopy open was restricted to speeds of less than 196 miles per hour. The value of the internal load coefficient C_{z_i} may be obtained from figure 12 for the various canopy positions.

The method outlined above has been applied to determine the canopy loads along the path AB–FA of an arbitrary design V–n diagram given in figure 17. In applying the results the computations were made for sea level with canopy closed and the engine operating at the thrust conditions shown in figure 4. The results are given in figure 18 where the full lines represent the external aerodynamic loads and the broken line the net aerodynamic loads; that is, internal loads have been taken into account. The net structural load may be obtained by subtracting the inertia load of 42 pounds per load factor.

The results shown and the computations made in preparing figure 18 indicate that insofar as vertical load is concerned the most severe condition occurs at the highest speed. The main contribution is from the C_{z_L} term of the equation, the other terms being simply in the nature of corrections. This result applies particularly to the canopy-closed position. A detailed comparison is not possible with other canopy positions since Mach number corrections are not available. An examination of the quantities involved indicates, however, that as the canopy is opened, the net vertical load changes from exploding to crushing. This change is due to the fact that as the canopy is opened the load contribution from the first term in the brackets of the equation decreases and that due to the last term increases. At any given speed, however, the vertical crushing load with the canopy open is smaller than the vertical exploding load with the canopy closed.

From the discussion on net canopy loads it appears that it would be safe to open the canopy at any speed; however, the center of pressure of these loads has not been determined. In this connection moment coefficients were calculated about the leading edge of the canopy for the vertical loads with power off. These results are presented in figure 19 as the center of pressure as a function of airplane lift coefficient. As the speed is increased in level flight the center of pressure moves forward; also, as the canopy is opened the center of pressure moves forward. It will be noted that the center of pressure will be approximately halfway between the supports at the present restricted speed of 196 miles per hour. Since the magnitude of the net load is reduced as the canopy is opened, loads on the front support will not be larger for the canopy opened than for the canopy closed unless the airplane is subjected to yawed flight.

SUMMARY OF RESULTS

External and internal pressure measurements have been made on a bubble-type canopy of a single-seated fighter airplane with power off and power on for four canopy positions. Within the limitations of the data the results show that:

1. Quantitative agreement exists between flight and full-scale wind-tunnel measurements.

2. The over-all effect of opening the canopy is to reduce the external negative pressure coefficients.

3. The external load coefficients increase in magnitude with an increase in lift coefficient. For all conditions tested this increase, whether with power off or power on, shows a linear variation with angle of attack.

4. Changes in pressure coefficients due to the effects of power result in both an increase in negative pressure coefficient and load asymmetry to the right for stations ahead of the maximum radius and to the left for stations aft of that point.

5. The vertical external load coefficient increases in magnitude due to the effects of Mach number. This increment is independent of the lift coefficient below the critical Mach number. Changes in other load components due to the effects of Mach number are of a second-order nature as compared to the magnitude of the vertical load coefficient changes.

6. The effects of distortion do not appear to be significant for this structure.

7. The center of pressure of the canopy moves forward with both an increase in speed in level flight and opening the canopy.

8. The load coefficients obtained from the pressure measurements can be used to calculate net structural loads on the canopy of the airplane under operating conditions of altitude, power, speed, and load factor within the design V-n diagram.

Langley Aeronautical Laboratory
National Advisory Committee for Aeronautics
Langley Field, Va.

REFERENCES

1. Cocke, Bennie W., Jr., and Czarnecki, K. R.: Canopy Loads Investigation for the F6F-3 Airplane. NACA RM No. L6L23a, 1947.

2. Dexter, Howard E., and Rickey, Edward A.: Investigation of the Loads on a Conventional Front and Rear Sliding Canopy. NACA RM No. L7D04, 1947.

3. Cocke, Bennie W., Jr.: Investigation of the Loads on a Typical Bubble-Type Canopy. NACA RM No. L7D07, 1947.

4. Danforth, Edward C. B., III, and Reeder, John P.: Flight Measurements of Internal Cockpit Pressures in Several Fighter-Type Airplanes. NACA TN No. 1173, 1947.

5. Wright, Ray H.: Estimation of Pressures on Cockpit Canopies, Gun Turrets, Blisters, and Similar Protuberances. NACA ACR No. L4E10, 1944.

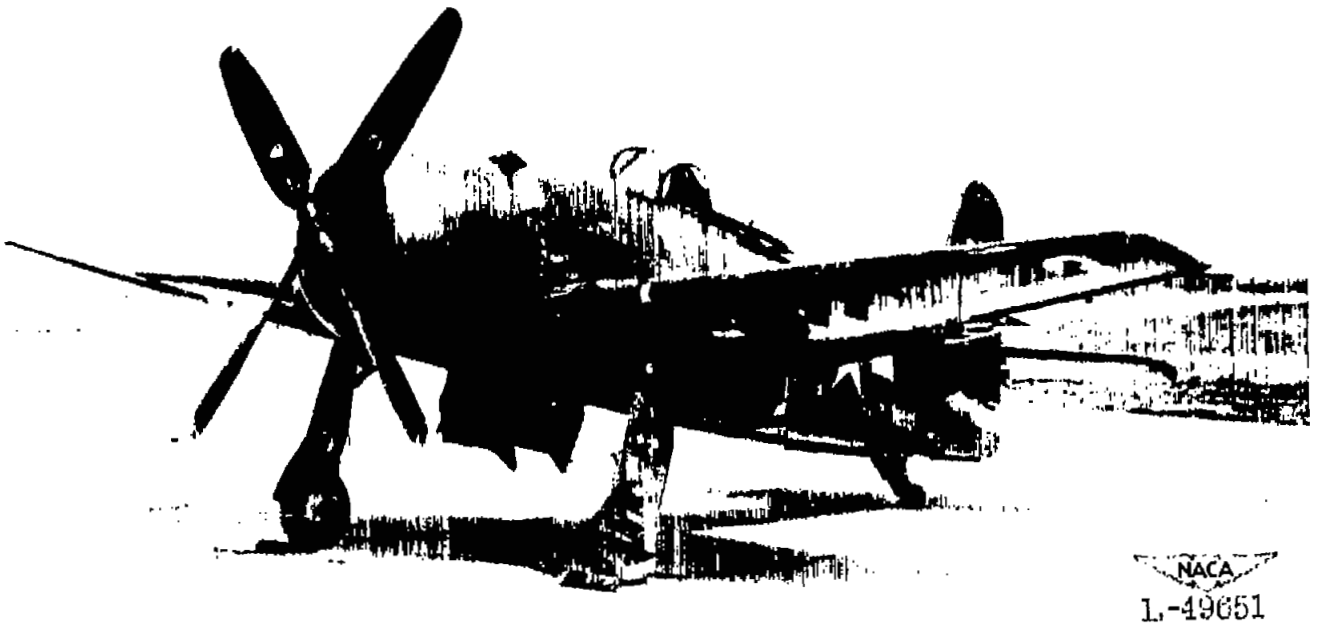

Figure 1.- Three-quarter front view of test airplane.

Figure 2.- Test-airplane canopy closed.

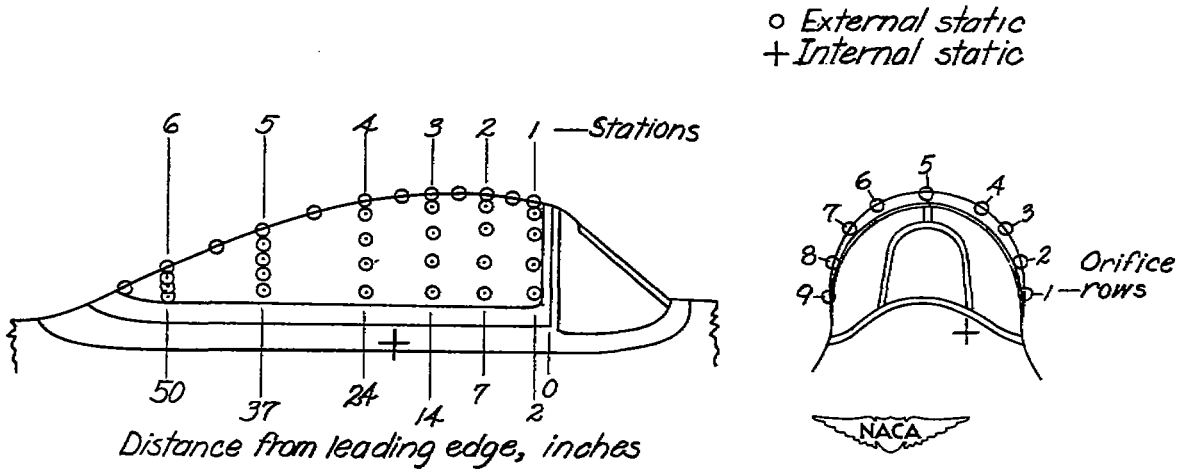

Figure 3.- Pressure-measurement station locations for the bubble-type canopy.

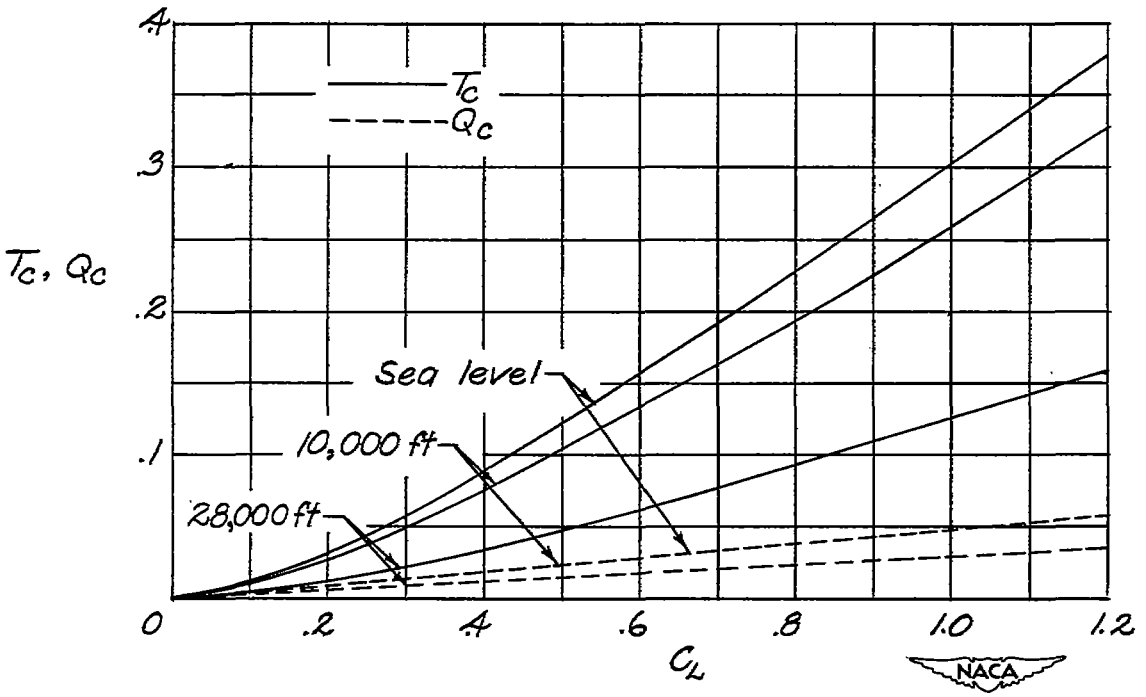

Figure 4.- Variation of thrust and torque coefficient for the airplane with lift coefficient for normal rated power and standard conditions. W/S = 37.7 pounds per square foot.

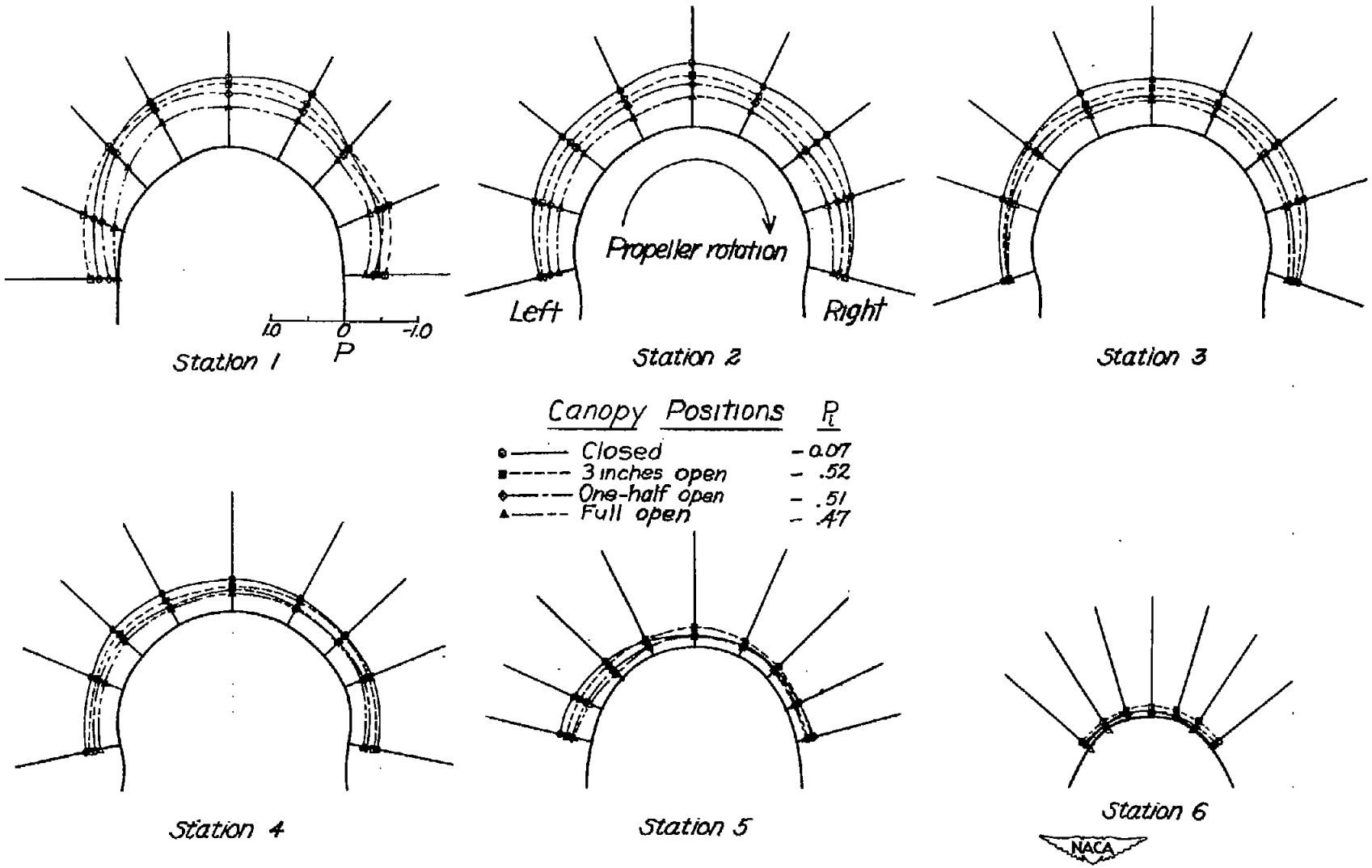

(a) Flight tests, M ≈ 0.30.

Figure 5.- Pressure distributions over the canopy of the test airplane for four canopy positions, power off, $C_L = 1.18$.

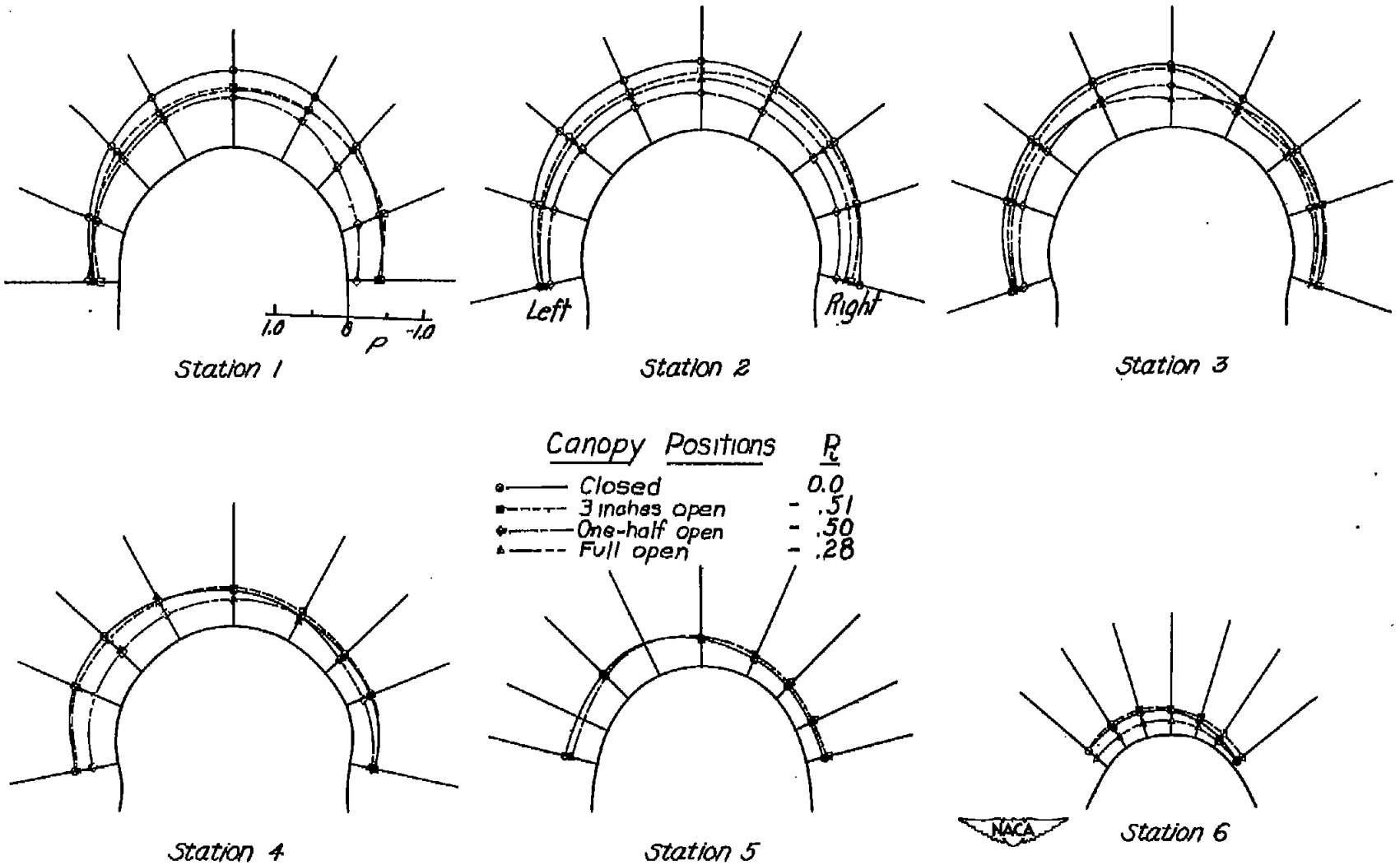

(b) Full-scale-tunnel tests.

Figure 5.- Concluded.

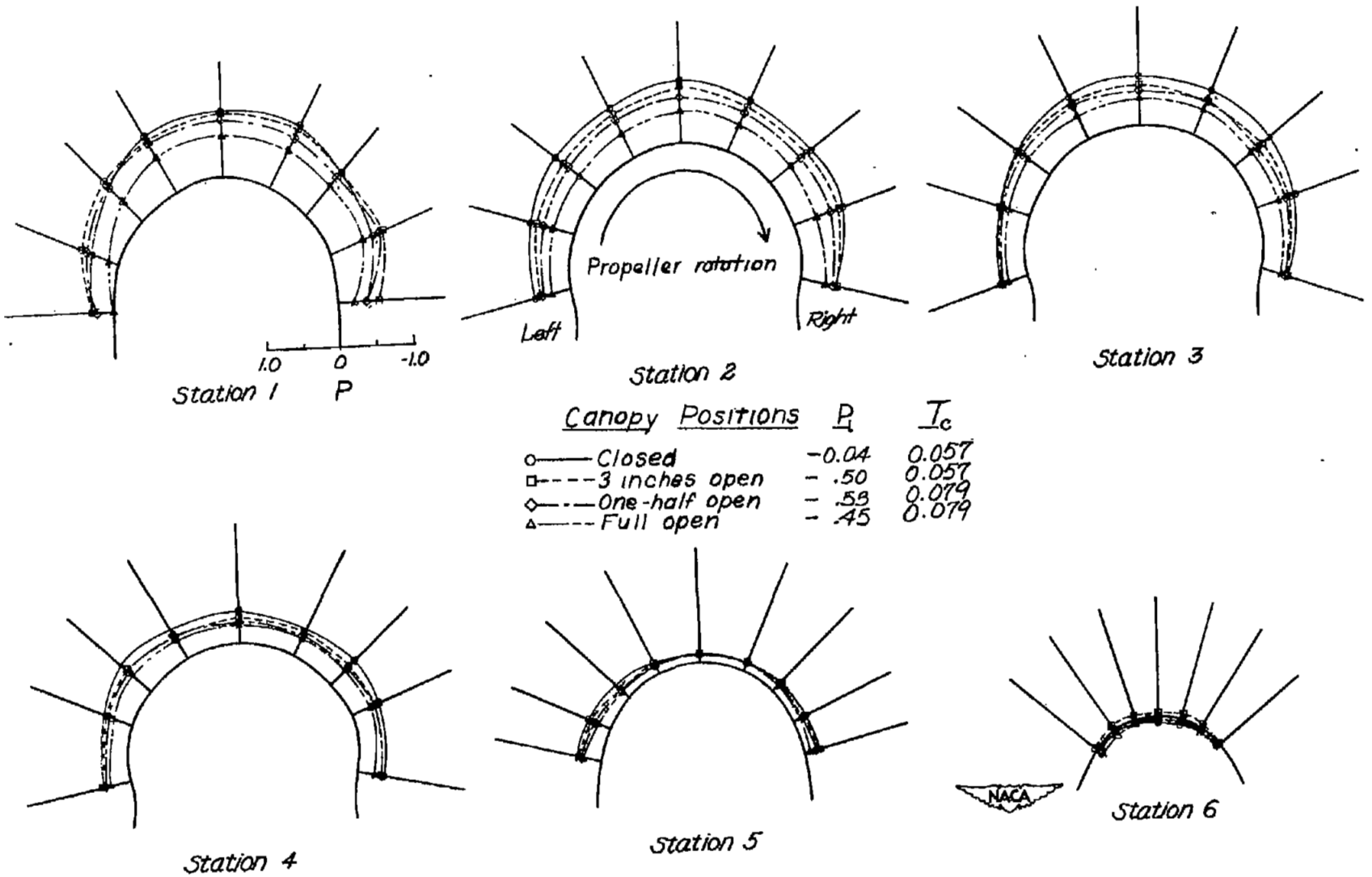

Canopy Positions	P_t	T_c
Closed	-0.04	0.057
3 inches open	- .50	0.057
One-half open	- .58	0.079
Full open	- .45	0.079

(a) Flight tests, M ≈ 0.30.

Figure 6.- Pressure distributions over the canopy of the test airplane for four canopy positions, power on, C_L = 0.50.

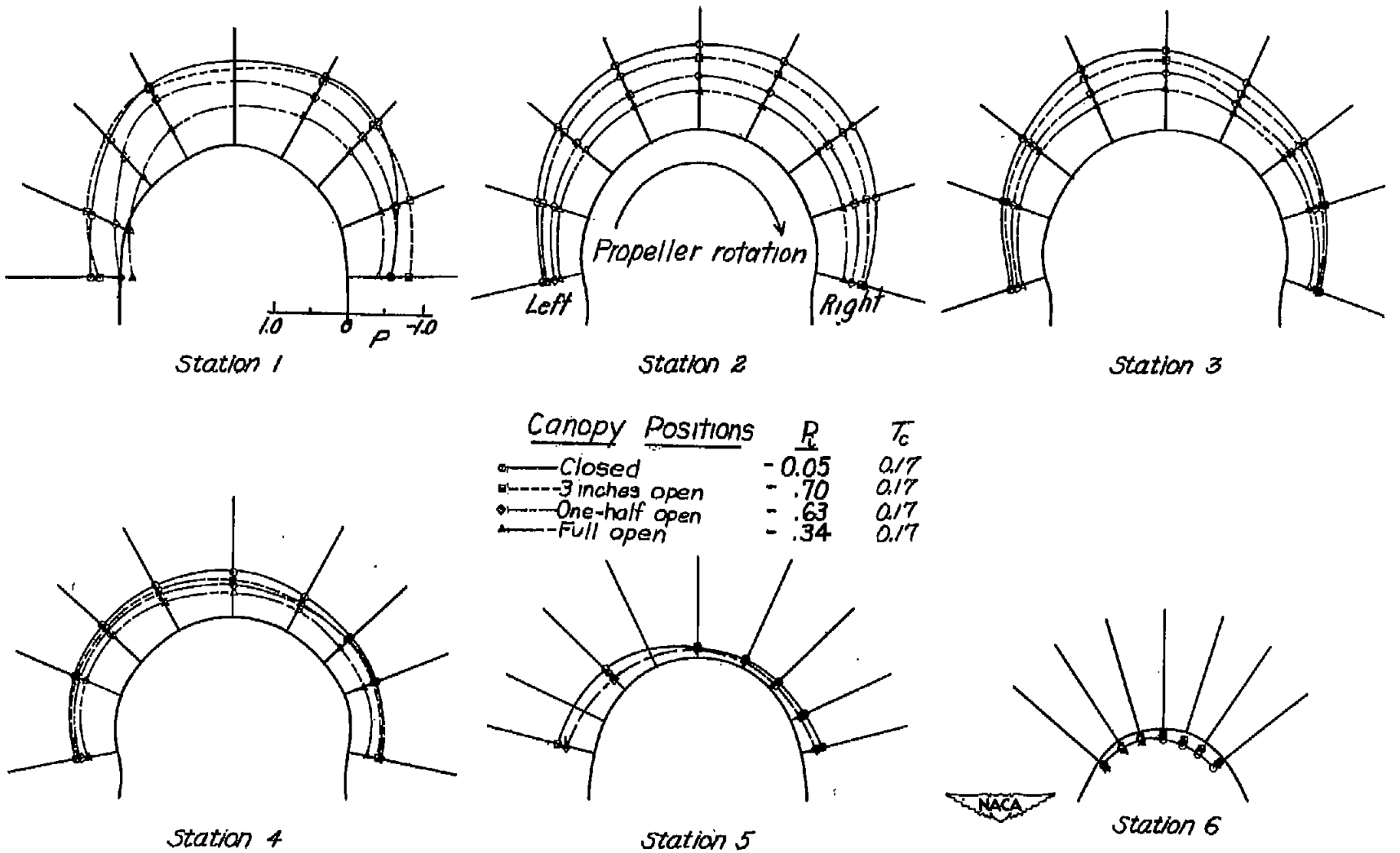

(b) Full-scale-tunnel tests.

Figure 6.- Concluded.

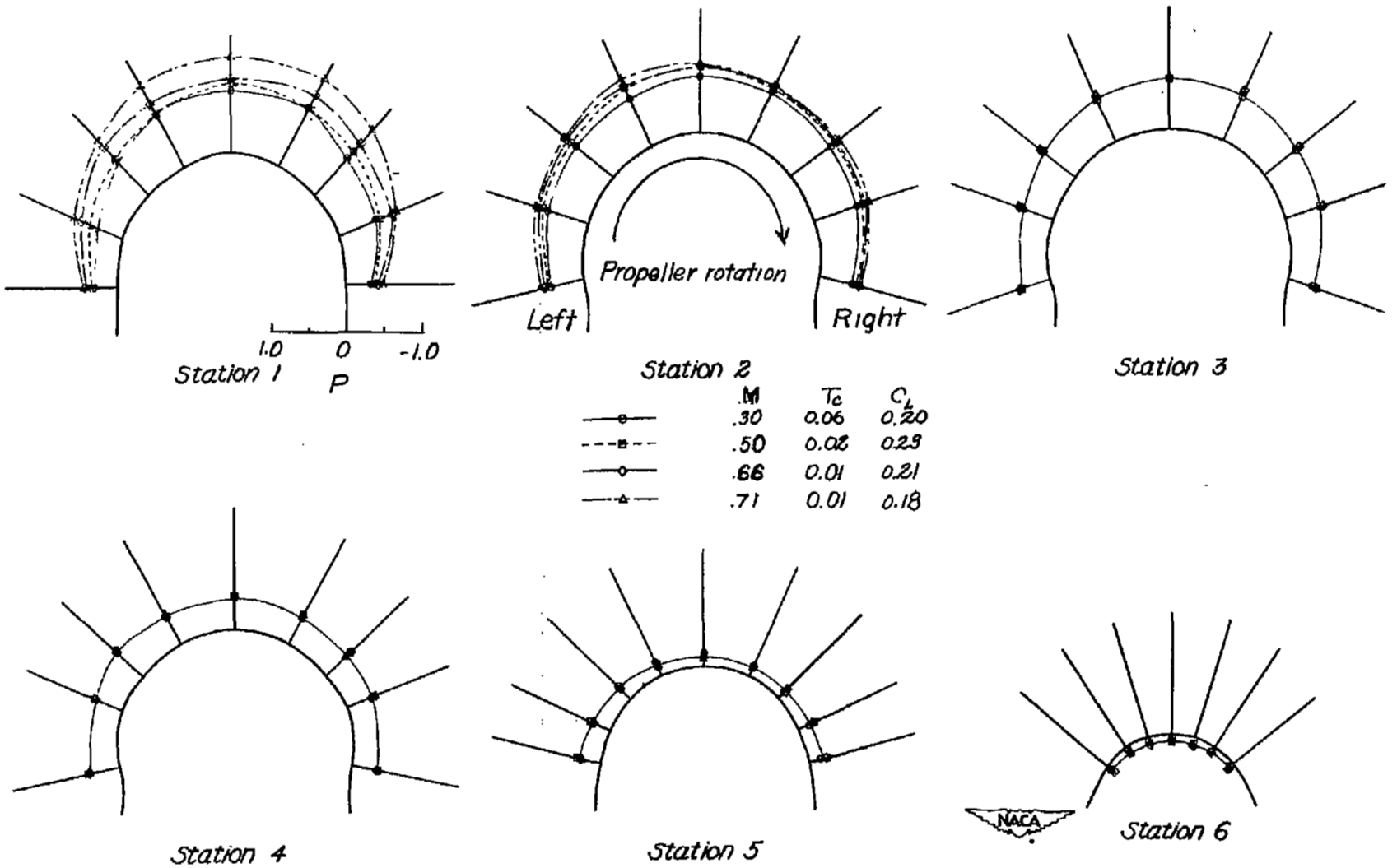

Figure 7.- Effect of Mach number on the pressure distributions over the canopy of the test airplane with canopy closed and power on.

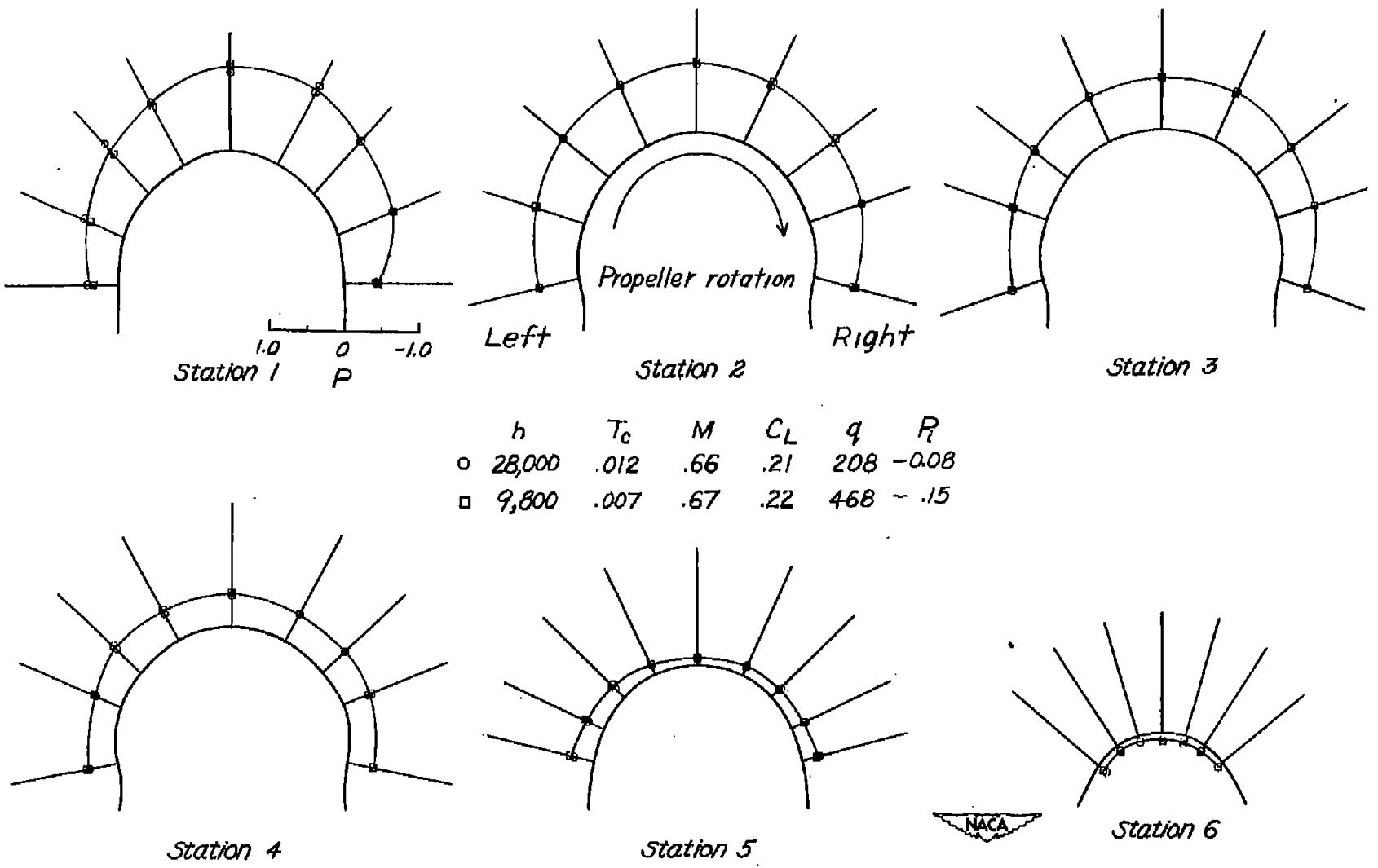

Figure 8.- Effect of distortion on the pressure distributions over the canopy of the test airplane.

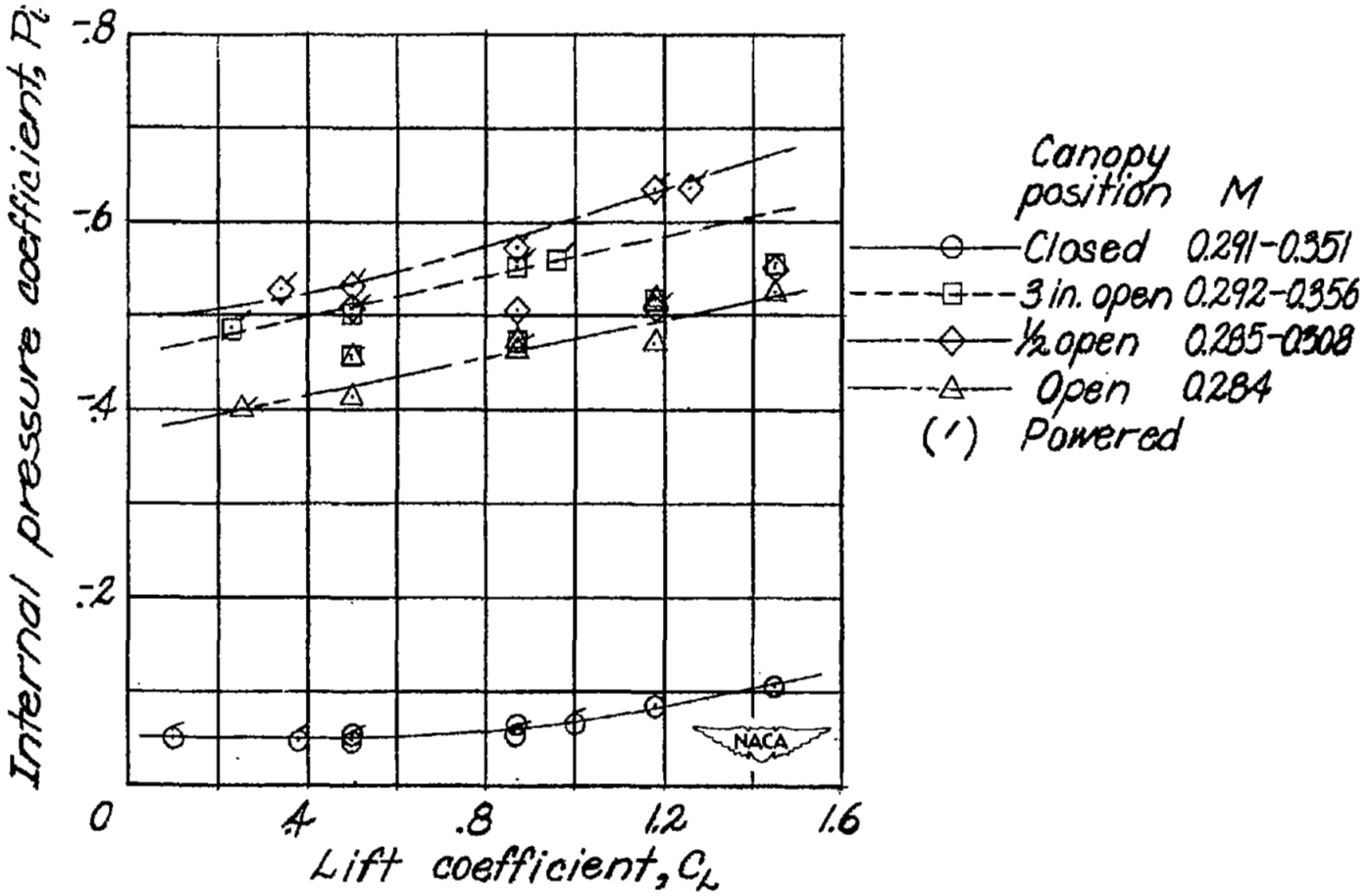

Figure 9.- Variation of internal pressure coefficient with lift coefficient and Mach number.

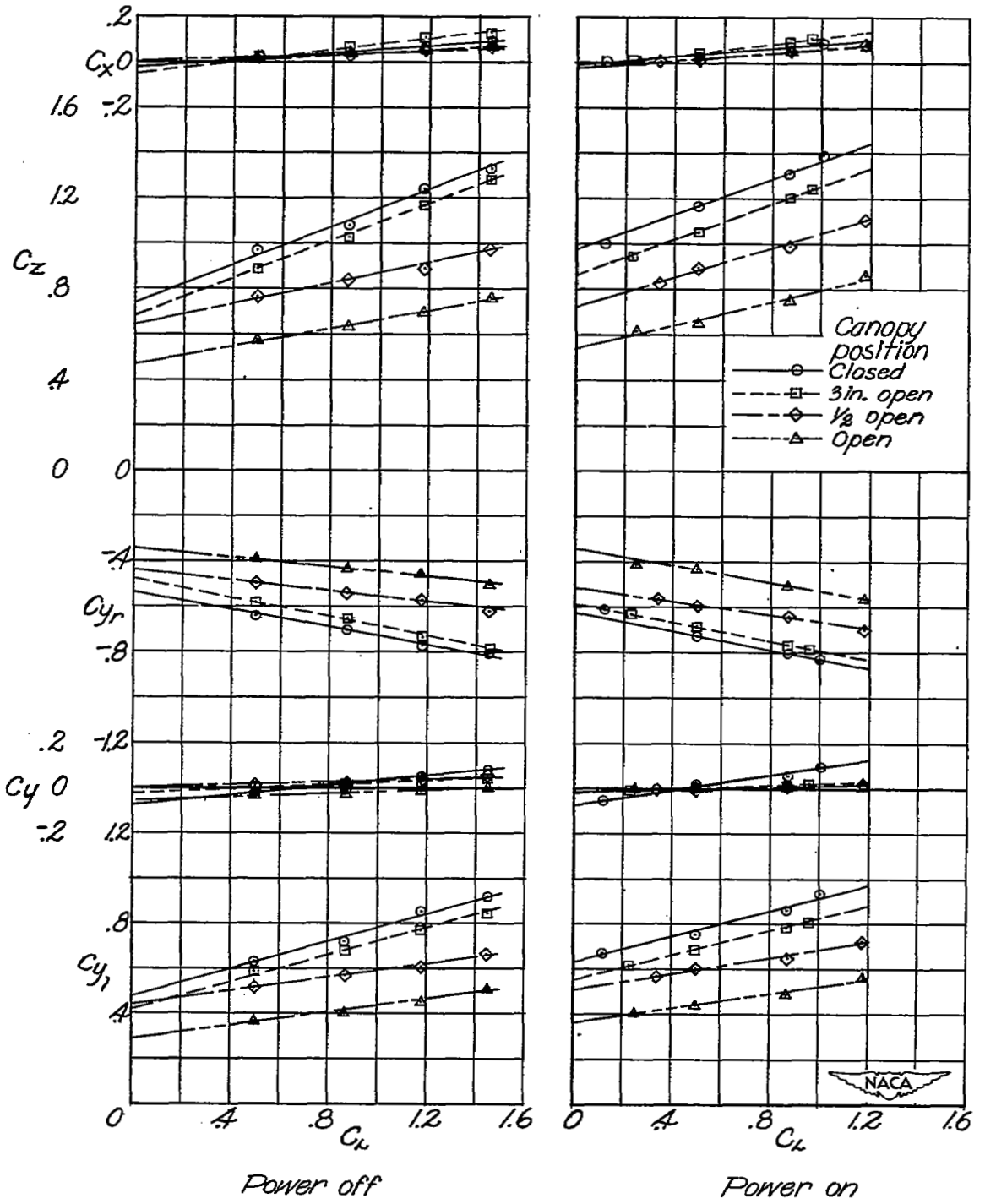

Figure 10.- Variation of load coefficient with lift coefficient and power for four canopy positions.

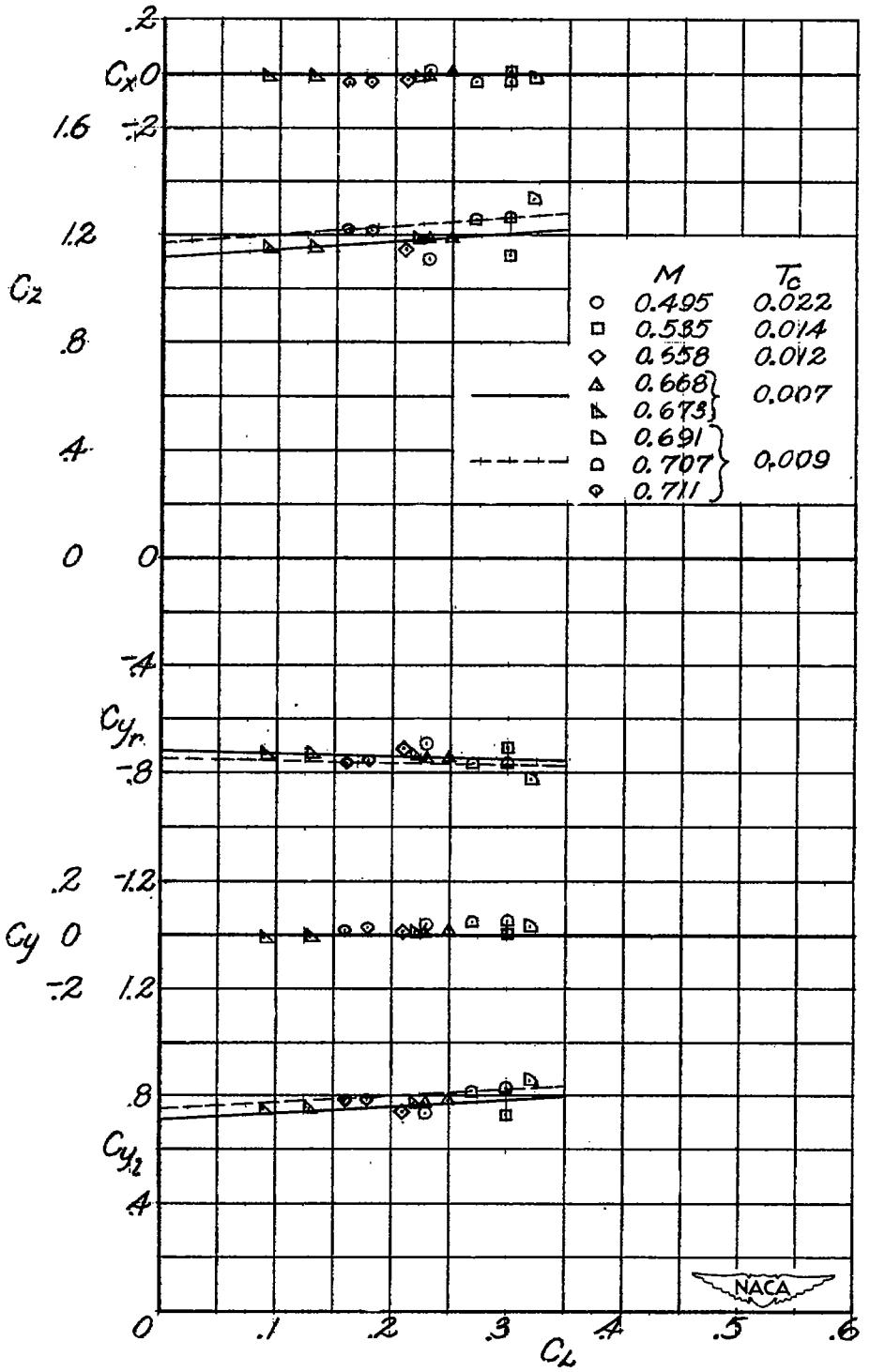

Figure 11.- Variation of load coefficient with lift coefficient and Mach number for canopy closed and power on.

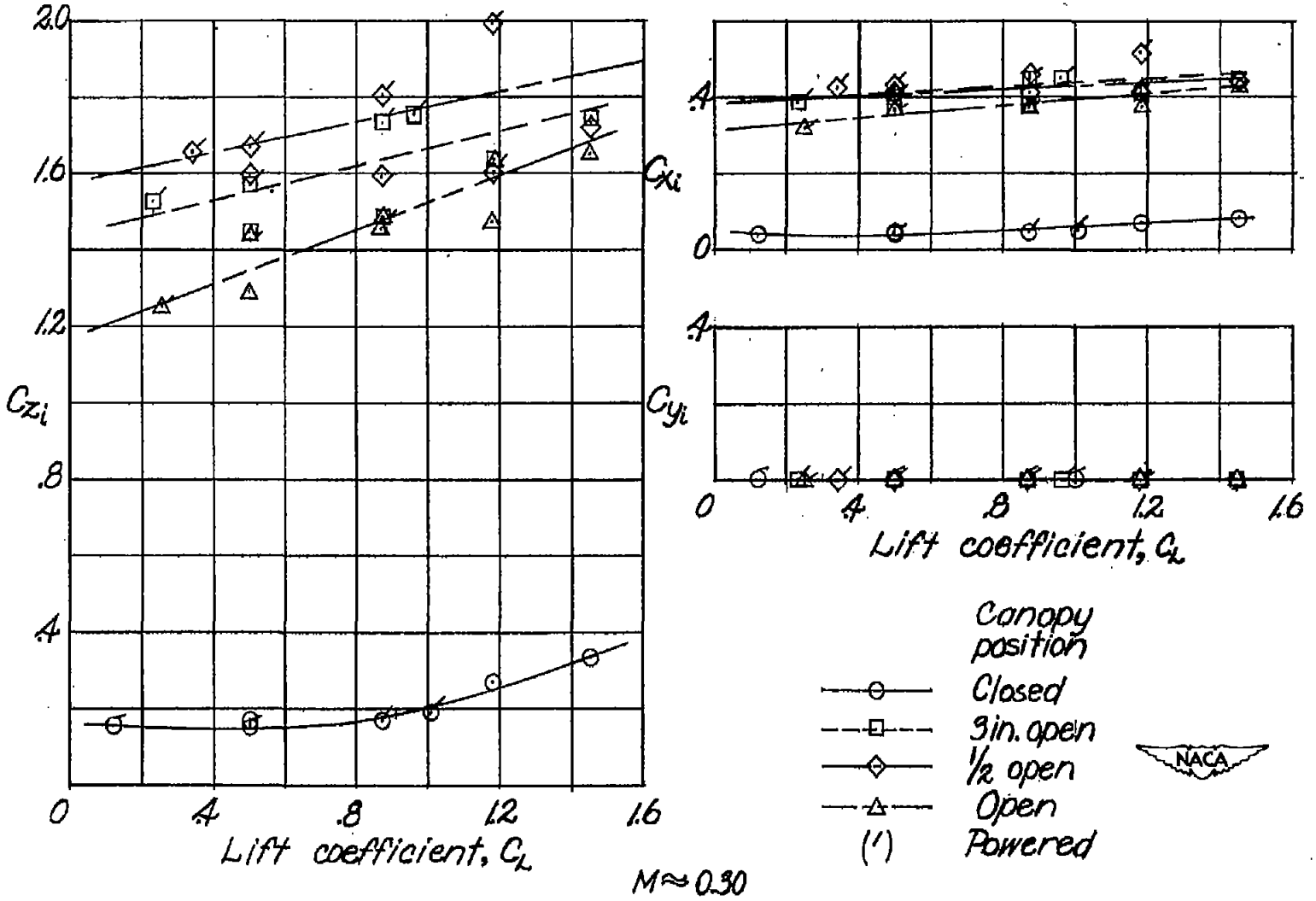

Figure 12.- Internal load coefficient as a function of lift coefficient and power for four canopy positions.

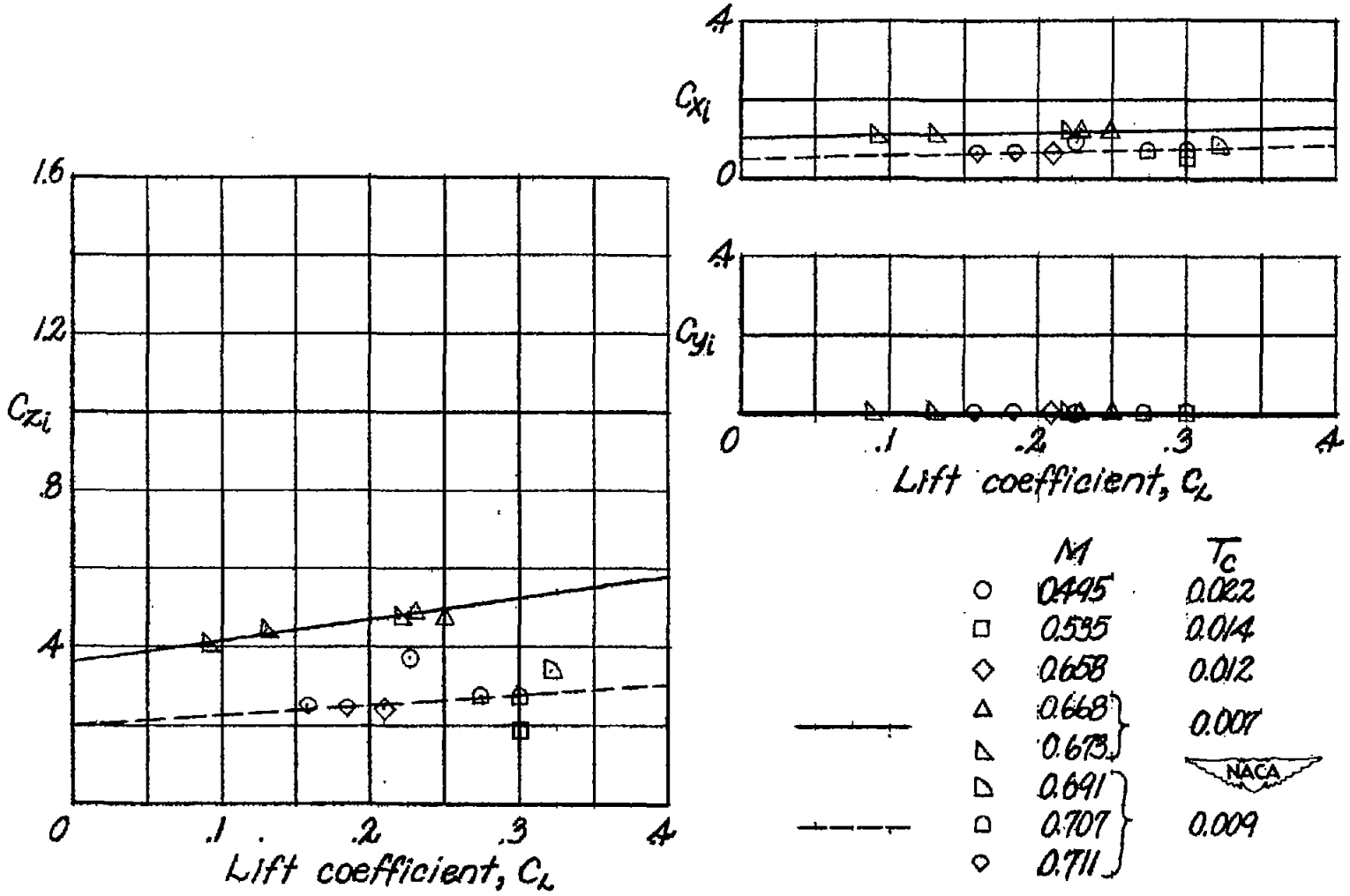

Figure 13.- Internal load coefficient as a function of lift coefficient and Mach number for canopy closed and power on.

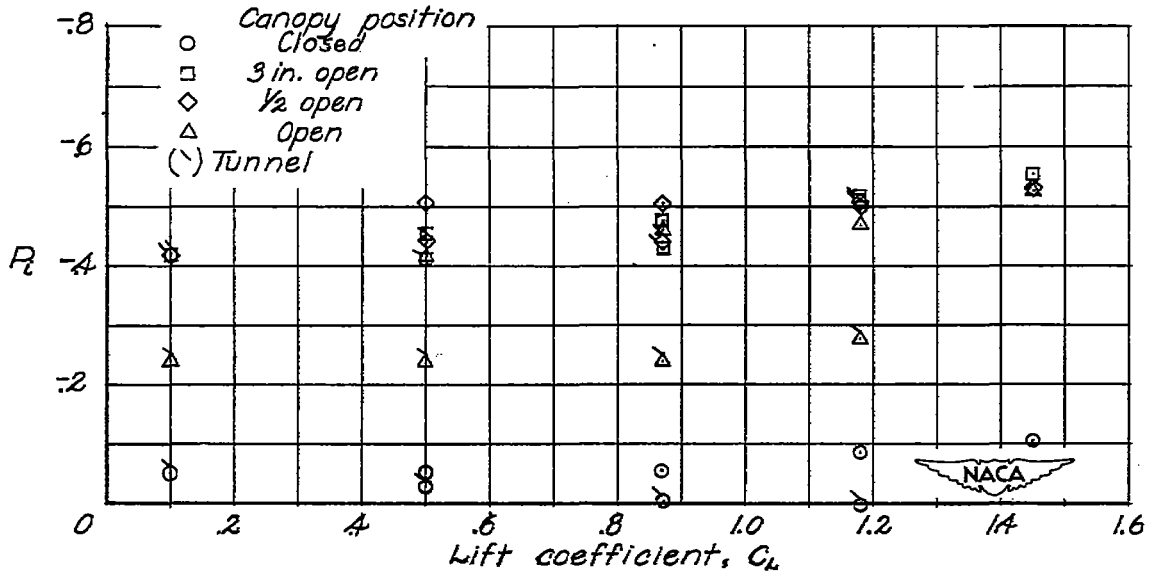

Figure 14.- Variation of internal pressure coefficient with lift coefficient from flight and full-scale-tunnel tests for different airplanes, power off.

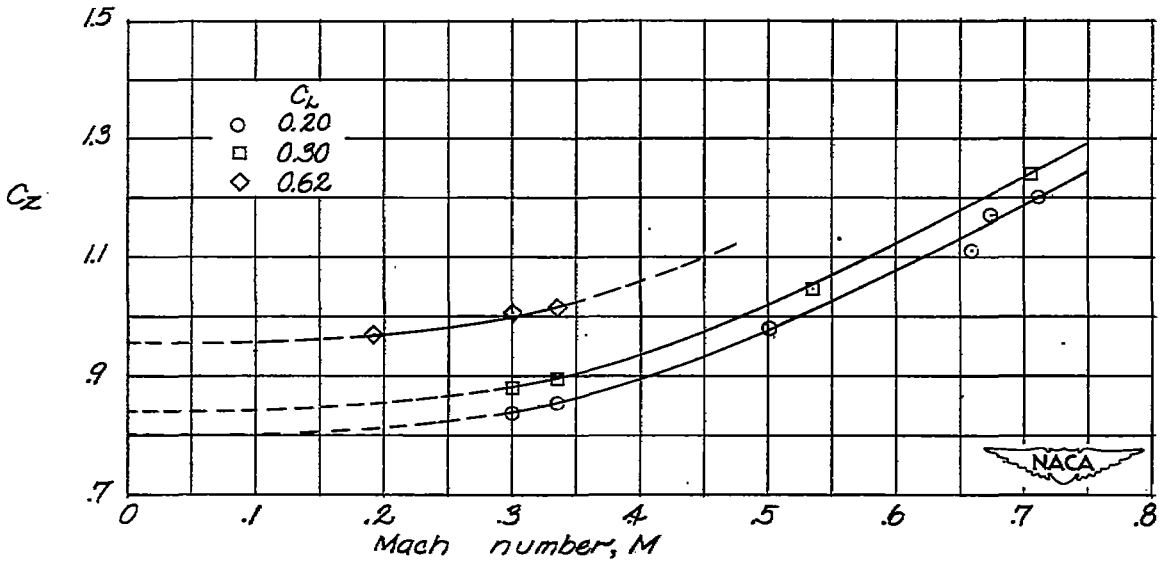

Figure 15.- Variation of vertical load coefficient with Mach number for canopy closed and power off.

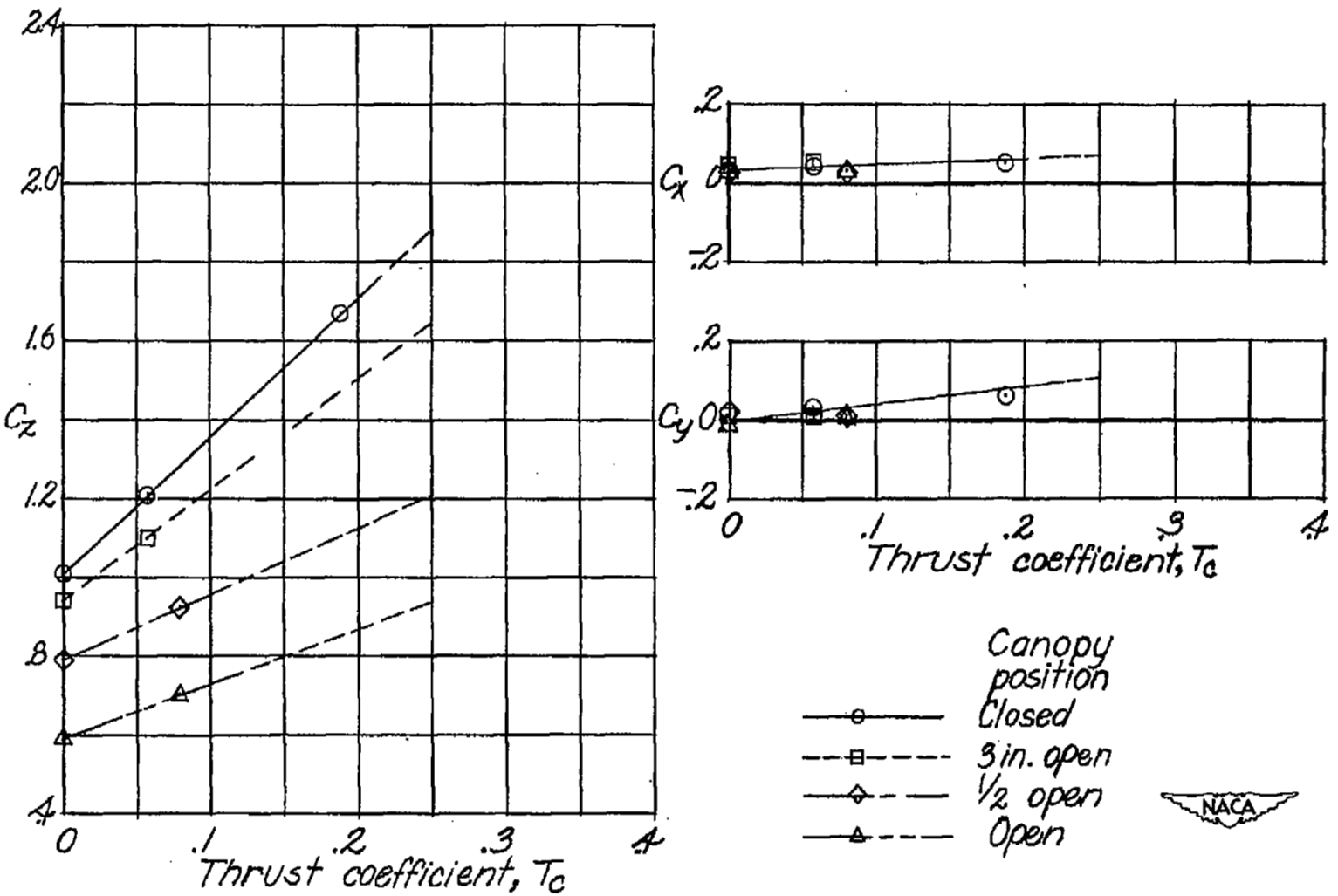

Figure 16.- Load coefficient as a function of thrust coefficient for the canopy of the test airplane. C_L = 0.62.

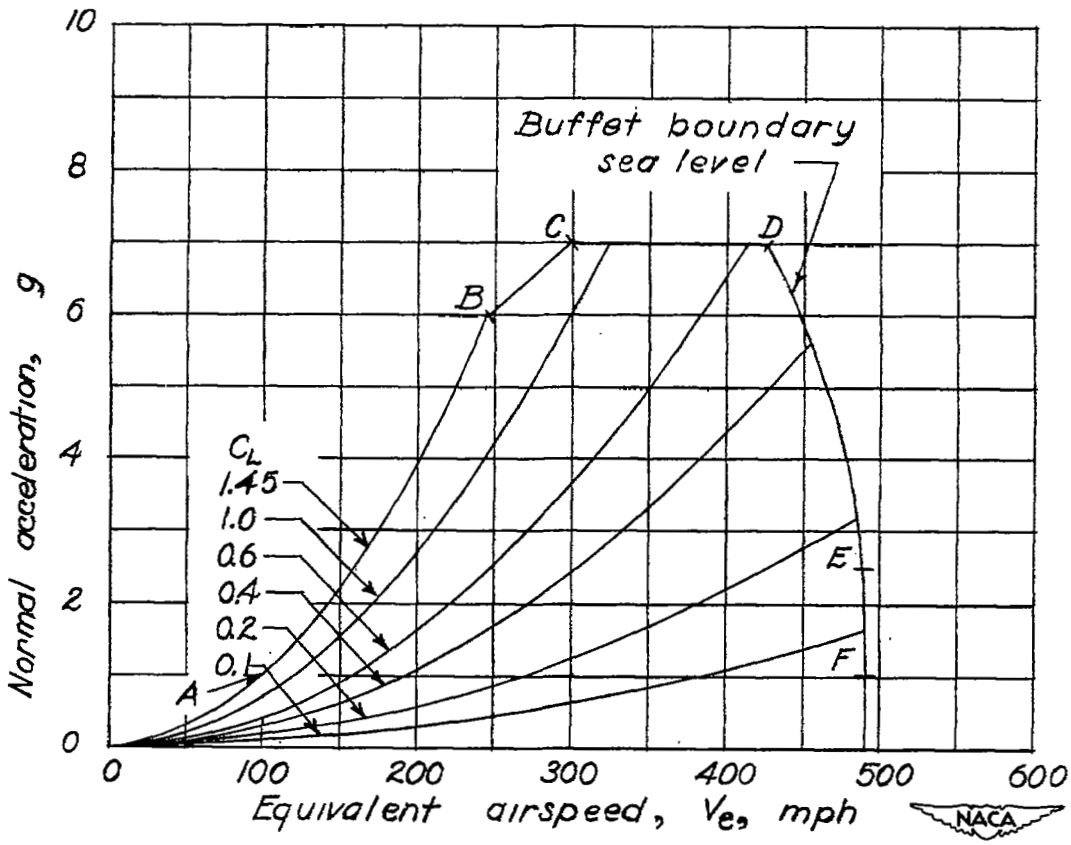

Figure 17.- Arbitrary V-n diagram for test airplane with wing loading of 37.7 pounds per square foot, sea level.

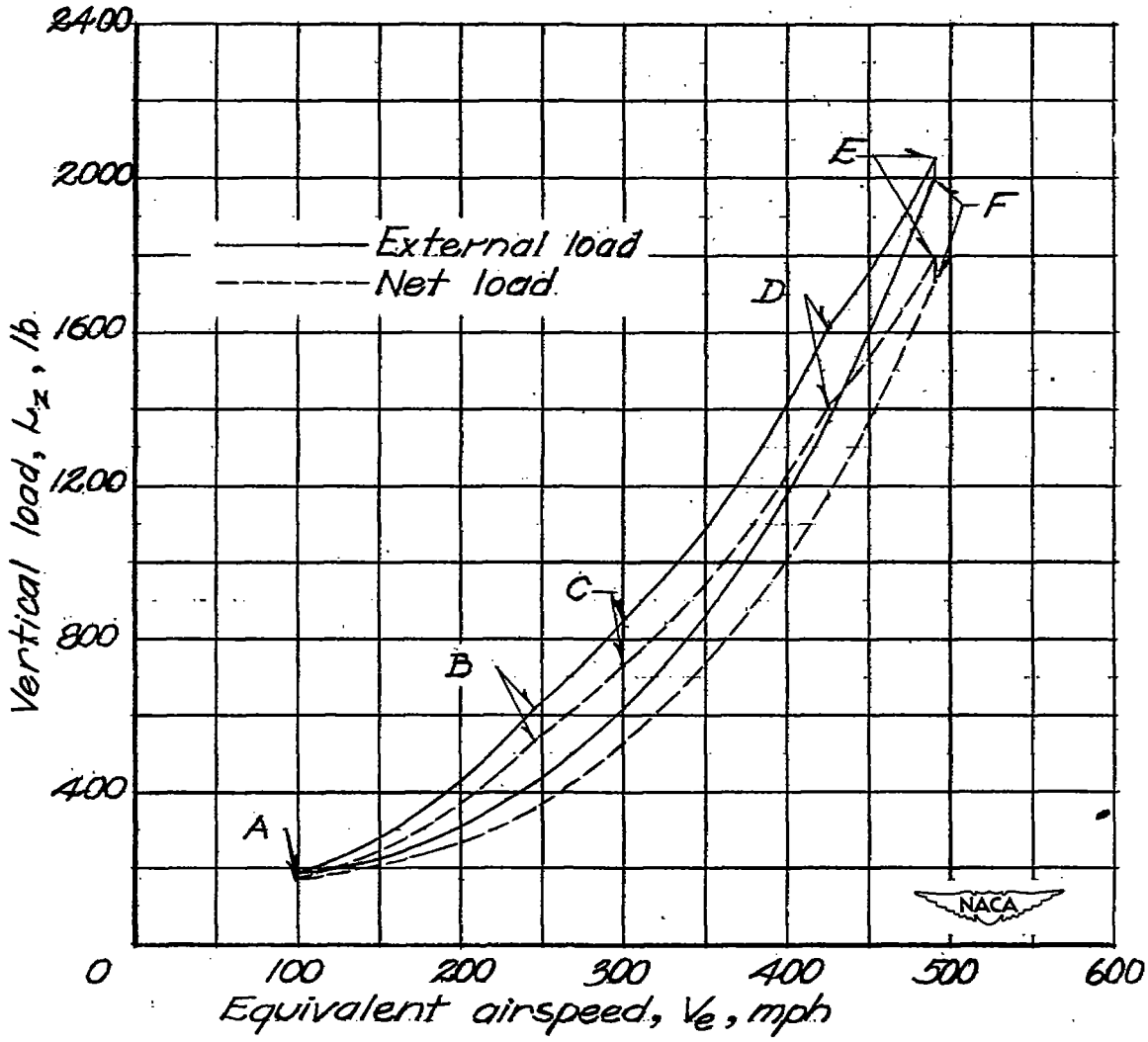

Figure 18.- Vertical canopy loads for test airplane encountered traversing the envelope of the V-n diagram. Rated power at sea level. Canopy closed.

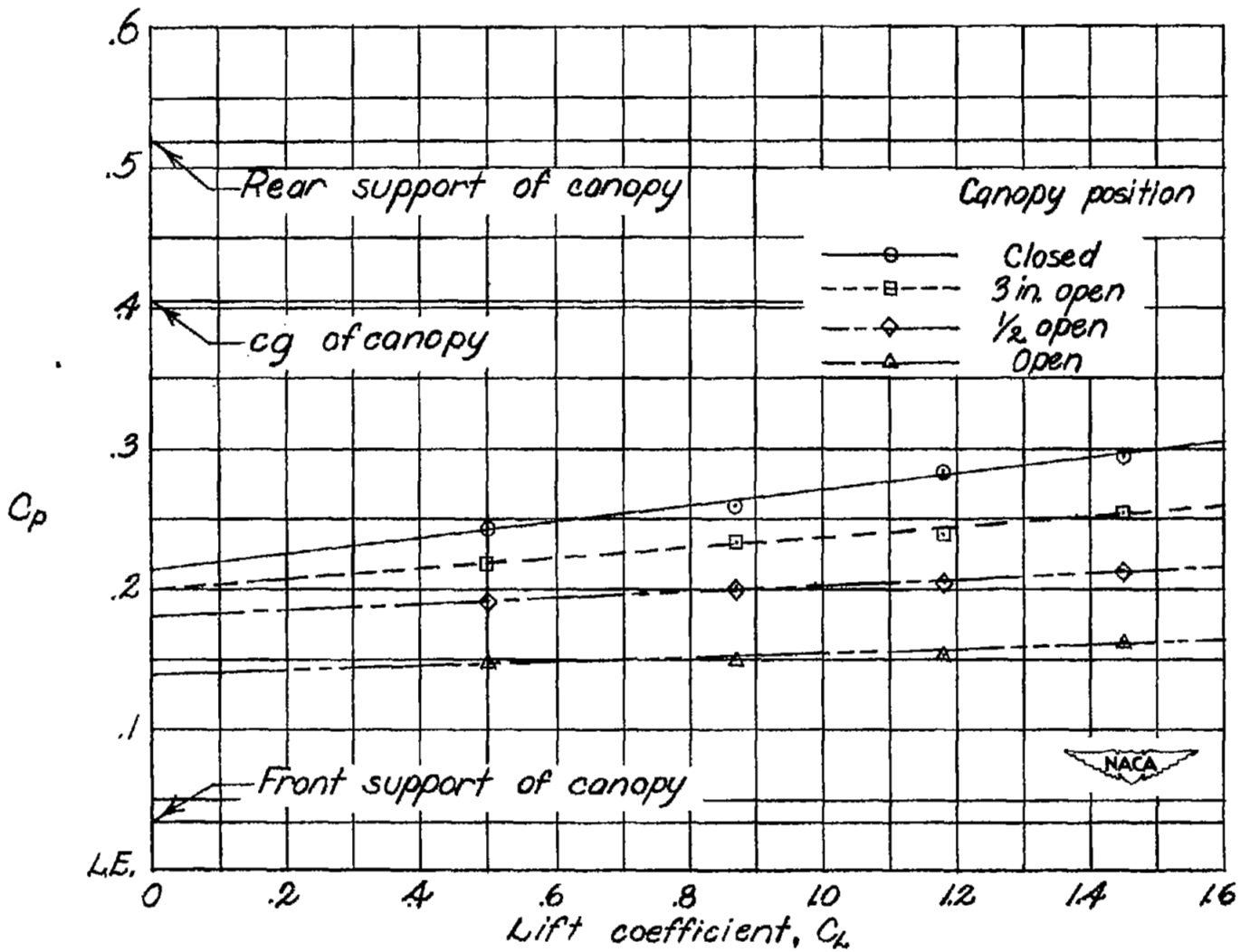

Figure 19.- Variation of center of pressure for bubble-type canopy with lift coefficient for power off, M ≈ 0.30.